Journal of
Plankton Research

plankt.oxfordjournals.org

Featured Article

J. Plankton Res. (2013) 35(5): 939–956. First published online June 4, 2013 doi:10.1093/plankt/fbt056

Relationships between phytoplankton thin layers and the fine-scale vertical distributions of two trophic levels of zooplankton

ADAM T. GREER[1]*, ROBERT K. COWEN[1], CEDRIC M. GUIGAND[1], MARGARET A. MCMANUS[2], JEFF C. SEVADJIAN[2] AND AMANDA H.V. TIMMERMAN[2]

[1]ROSENSTIEL SCHOOL OF MARINE AND ATMOSPHERIC SCIENCE, MARINE BIOLOGY AND FISHERIES, UNIVERSITY OF MIAMI, 4600 RICKENBACKER CSWY, MIAMI, FL 33149, USA AND [2]DEPARTMENT OF OCEANOGRAPHY, UNIVERSITY OF HAWAII AT MANOA, 1000 POPE ROAD, HONOLULU, HI 96822, USA

*CORRESPONDING AUTHOR: agreer@rsmas.miami.edu

Received February 19, 2013; accepted May 9, 2013

Corresponding editor: Roger Harris

Thin layers of phytoplankton are well documented, common features in coastal areas globally, but little is known about the relationships of these layers to higher trophic levels. We deployed the *In Situ* Ichthyoplankton Imaging System (ISIIS) to simultaneously quantify the three trophic levels of plankton, including phytoplankton, primary consumers (copepods and appendicularians) and secondary consumers (gelatinous zooplankton). Over a 2-week sampling period, phytoplankton thin layers, primarily composed of *Pseudo-nitzschia* spp., were common on two of the five sampling days. Imagery showed copepods aggregating in zones of lower chlorophyll-*a* fluorescence, while appendicularians were more common at greater depths and higher chlorophyll-*a* levels. All gelatinous zooplankton generally increased in abundance with depth. *Bolinopsis* spp. ctenophores underwent a 'bloom,' and they were the only species observed to aggregate within phytoplankton thin layers. The vertical separation between copepods, phytoplankton and gelatinous zooplankton suggests that copepods may use the surface waters as a predation refuge, only performing short migrations into favorable feeding zones where gelatinous predators are much more abundant. Thin layers containing dense diatom aggregates obstruct light reaching deeper waters (>10 m), which may allow gelatinous zooplankton to avoid visual predation as well as improve the effectiveness of contact predation with copepod prey.

KEYWORDS: plankton imaging; thin layers; ctenophores; copepods; appendicularians

INTRODUCTION

Thin layers are dense aggregations of phytoplankton or zooplankton spanning a few centimeters to meters in depth and sometimes several kilometers horizontally (Dekshenieks *et al.*, 2001; McManus *et al.*, 2003). The concentrations of organisms within thin layers can be orders of magnitude greater than above or below the layer (Donaghay *et al.*, 1992), and persist on time scales of hours to days depending upon physical, chemical and biological conditions (Sullivan *et al.*, 2010). Thin layers are of interest ecologically because they may serve as zones of enhanced biological interactions in the vertical dimension (Alldredge *et al.*, 2002), much like fronts do in the horizontal, with the trophic impact of a thin layer increasing in relation to its temporal persistence (Cowles *et al.*, 1998). As thin layers can occur in a variety of marine systems including estuaries (Donaghay *et al.*, 1992), coastal shelves (Cowles and Desiderio, 1993) and fjords (Holliday *et al.*, 1998; Dekshenieks *et al.*, 2001; Alldredge *et al.*, 2002), they may be important contributors to community structure in shallow water environments.

Trophic interactions in relation to phytoplankton thin layers are influenced by the degree of spatial overlap between thin layers, grazers and zooplankton predators. While it may seem that grazers would seek an aggregated food source within thin layers, several studies have produced counter-intuitive results where grazers were found to spend a majority of time just outside of a thin layer (Bochdansky and Bollens, 2004; Benoit-Bird *et al.*, 2010; Talapatra *et al.*, 2013). One possible explanation for these observations is that zooplankton predators (including gelatinous zooplankton) may influence the distribution of grazers through predation or modification of grazer behavior. Linking the distribution of phytoplankton, zooplankton and gelatinous zooplankton aggregations is challenging due to sampling limitations. For example, the relative positioning of different zooplankton taxa in relation to phytoplankton thin layers is poorly described (Holliday *et al.*, 1998, 2003, 2010) because it is difficult or impossible to distinguish acoustic returns from organisms of similar acoustic impedance (typically similarly sized). Further, common gelatinous zooplankton are extremely difficult to sample with traditional net sampling systems [e.g. MOCNESS (Wiebe *et al.*, 1976)], which destroy fragile gelatinous bodies. Gelatinous zooplankton are also thought to have low acoustic detectability, except for large (>10 cm) specimens (Monger *et al.*, 1998; Brierley *et al.*, 2005), thus their association with thin layers and grazers was not known prior to the present study.

Although gelatinous zooplankton are known to aggregate within temperature discontinuities (Arai, 1976; Graham *et al.*, 2001), field studies relating gelatinous zooplankton distributions to the well-understood physical processes of thin layer formation are limited. The frontal zone at the edge of the upwelling shadow has been implicated as a retention mechanism for the large (30 cm bell diameter) scyphomedusa *Chrysaora fuscescens*, with highest concentrations located near the thermocline (Graham, 1993). Hydromedusae have been found to be abundant in Monterey Bay (Raskoff, 2002) and consistently aggregate in salinity discontinuities, regardless of whether or not prey is present indicating that they may use physical cues to aggregate there (Frost *et al.*, 2010).

In Monterey Bay, CA, USA, thin layers of phytoplankton typically form during upwelling favorable (northwesterly) winds when the northern (sheltered) region of the bay tends to be thermally stratified (Graham and Largier, 1997; McManus *et al.*, 2008). The upwelling season spans between the months of March–October (Pennington and Chavez, 2000). During upwelling events, cold, nutrient-rich filaments cross the mouth of the bay (Rosenfeld *et al.*, 1994) and a cyclonic gyre, known as the 'upwelling shadow,' forms in the northeastern part of the bay. When present, the upwelling shadow increases the surface water residence time in the bay (Breaker and Broenkow, 1994; Graham and Largier, 1997). Water in the upwelling shadow is sheltered from the winds, which results in decreased mixing, and diurnal heating results in high thermal stratification (Graham, 1993). These characteristics provide optimal conditions for thin layer formation. Density discontinuities formed via thermal stratification may serve as a mechanism to slow the sinking rate of particles, creating thin phytoplankton layers of non-motile organisms such as diatoms (MacIntyre *et al.*, 1995; Alldredge *et al.*, 2002). When the upwelling winds subside or reverse direction, *i.e.* 'relaxation events,' surface waters in the upwelling shadow zone are advected from the bay to the northwest within 2–3 days if the event persists (Woodson *et al.*, 2009). Under these conditions, California current waters, characterized by relatively warm temperatures, low salinity and low nutrient concentrations (Rosenfeld *et al.*, 1994; Ramp *et al.*, 2005; Ryan *et al.*, 2008, 2009), are advected towards shore to replace exiting waters, disrupting the stratified conditions favorable to thin layer formation.

To elucidate the trophic effects of phytoplankton thin layers and directly sample the gelatinous community, we deployed a towed *In Situ* Ichthyoplankton Imaging System (ISIIS) (Cowen and Guigand, 2008) to synoptically sample zooplankton abundance and related environmental parameters (including chlorophyll-*a* fluorescence) in northern Monterey Bay. The goals of this study were (i) to describe the environmental conditions and their relationship to thin layers, (ii) to relate fine scale changes in abundance of different zooplankton taxa to environmental conditions and (iii) to compare and contrast the fine-scale vertical distributions of three distinct planktonic trophic levels (phytoplankton, primary consumers and gelatinous zooplankton), their relationship to physical discontinuities and the implications for predator/prey interactions.

METHOD

Study site and sampling period

Monterey Bay is an open embayment located on the central coast of California. The study area was in the northeastern part of the bay where the upwelling shadow tends to form during active upwelling (Fig. 1). All sampling was conducted over 5 days between 28 June and 7 July 2010 in conjunction with a large physical oceanographic study investigating lateral mixing on the inner shelf (Woodson *et al.*, in revision).

Moored vertical profiler and wind data

To continuously monitor hydrographic and chlorophyll-*a* fluorescence variability in northern Monterey Bay waters, an autonomous vertical profiler (Brooke Ocean Technology SeaHorse) was deployed on the 20 m isobath in the center of the ISIIS sampling array at 36.9325°N 121.9244°W. The SeaHorse provided profiles every 30 min from near-surface to near-bottom with a Sea Bird 19 CTD, a Sea Bird 43 Oxygen sensor and a Wet Labs WetStar fluorometer with a sampling frequency of 4 Hz. For the period between 5 July and 7 July 2010, the SeaHorse collected data on 54% of its profiles. Some data loss occurred near the end of deployment due to issues with the gripper mechanism, creating gaps in the time series.

Regional scale wind forcing (and thus upwelling/relaxation conditions) was obtained using hourly averaged wind velocities from the National Data Buoy Center's buoy number 46042 located at 36.789°N122.404°W, ~51 km WSW from the profiling sites. The direction and magnitude of these winds indicate whether or not active upwelling was occurring.

Imaging system sampling

The ISIIS contains a Piranha II line scan camera from Dalsa with 68 μm pixel resolution, imaging plankton in the size range of 680 μm to 13 cm. The ISIIS uses a shadowgraph imaging technique, in which a collimated light source is projected across a sampled parcel of water, and the silhouettes created by the plankton blocking the light source are then captured by the camera (Cowen and Guigand, 2008). The ISIIS line scan camera shoots a continuous image at 36 000 scan lines per second, but parses the image into frames that correspond to a 13 × 13 cm area of view with a depth of field of *ca.* 35 cm, giving an individual image volume of 6.4 L. At the usual tow speed (2.5 ms^{-1}), 1 m^3 of water is sampled every 7.7 s. In addition to the camera system, ISIIS was equipped with motor actuated fins for depth control, a Doppler velocity log (600 micro, Navquest) and environmental sensors including a CTD (SBE49, Seabird Electronics) and fluorometer [ECO FL (RT), Wetlabs chlorophyll-*a* fluorescence]. All sensors sampled water <1 m above the imaging area at a rate of 2 Hz, and a correction was applied to address this offset.

The system was deployed in a 'tow-yo' fashion behind an 18 m research vessel, the R/V Shana Rae, running at a constant speed of 2.5 ms^{-1} through the water, with ~4–5 water column undulations per transect from the near surface to a maximum depth of ~18 m to stay at least 5 m from the bottom. A total of 10 transects (3 km each) centered over the 20 m isobath were performed on each day of sampling (Fig. 1), with the exception of 5 July, when only 5 transects were completed due to temporary technical issues. All sampling was conducted during the day except for samples on 30 June, which were collected at night. Due to the optical technique utilized by ISIIS, ambient light has no effect on image quality (Cowen and Guigand, 2008).

Thin layer identification

In the ISIIS profiles, thin layers of fluorescence were defined as in Sullivan *et al.* (Sullivan *et al.*, 2010), but the maximum layer thickness criterion was adjusted from <3 to <5 m (*sensu* Sevadjian *et al.*, submitted). The method by Sullivan *et al.* (Sullivan *et al.*, 2010) describes the intensity and thickness of the chlorophyll maximum in each fluorescence profile. ISIIS chlorophyll-*a* profiles were first smoothed using a low pass filter, and the first derivative was calculated to determine background fluorescence, layer thickness, and intensity. The depth of the fluorometer was calculated using the pressure sensor mounted on the upper pod of ISIIS and corrected for the minor physical offset and vehicle pitch.

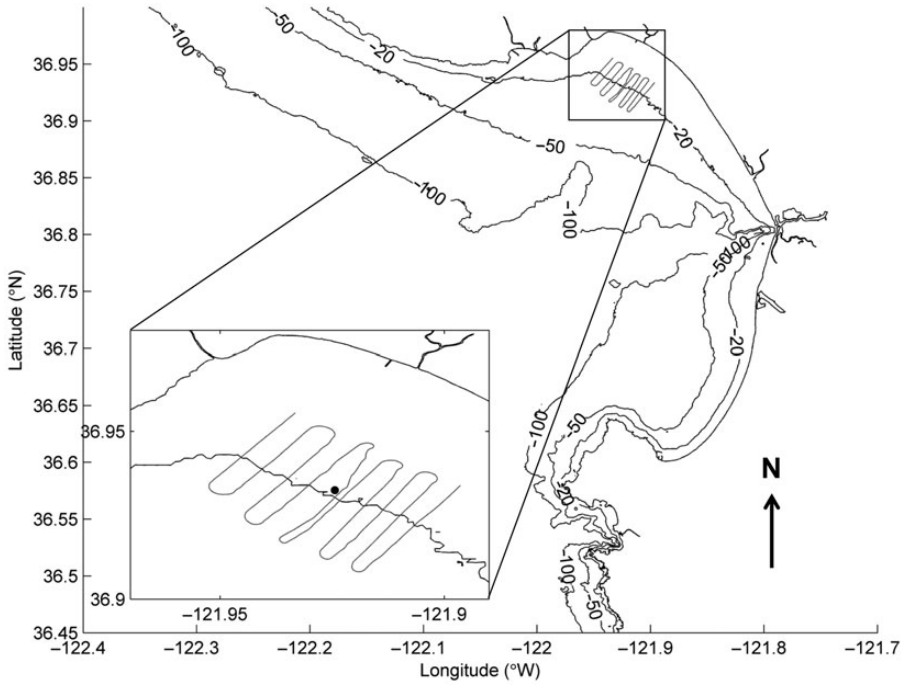

Fig. 1. Sampling track from each day of ISIIS sampling. Ten transects, each *ca.* 3 km long and 500 m apart, are shown in gray. The black dot on the inset figure shows the location of the SeaHorse profiler in the middle of the fifth transect.

Phytoplankton sampling

Water samples were taken to assess the phytoplankton community on the days of ISIIS sampling using a 5-L Aquatic Research Instruments discrete point water sampling bottle attached <0.2 m from the intake tubes on a high-resolution profiler on a separate small vessel. The bottle was triggered using real-time depth and chlorophyll-*a* fluorescence activity, with samples taken near surface ($\sim$3 m), within the chlorophyll maximum and below the chlorophyll maximum ($>$15 m). The bottle samples were stored on ice and gently mixed before analysis in the laboratory within 5 h of returning from the field. Phytoplankton were counted and identified to genus using a PhycoTech 0.066 mL phytoplankton counting cell at 40$\times$ magnification and a Zeiss A1 Axoioscope. Triplicates were performed for each sample and averaged.

Image data analysis

ISIIS images were viewed using the VisionNow software (Boulder Imaging, Inc.), and a standard 'flat-fielding' transformation was applied to remove background noise from each image. For quantification of gelatinous zooplankton, three vertical profiles from each of 10 daily transects were examined (30 profiles on each sampling day, 15 profiles on 5 July). The profiles were approximately evenly spaced across the study area ($\sim$1 km separation) and corresponded to different sections of the transect (offshore, middle and inshore). We refer to these units as 'profiles' even though they spanned a horizontal range of $\sim$300 m and an average depth of 15 m ($\sim$5 m above bottom). Gelatinous zooplankton were identified to genus or species level. Identification of the ctenophores and siphonophores was verified by experts in the field.

Measurements of length and angle of swimming orientation were made for a subset of ctenophore specimens ($n = 225$ for *Pleurobrachia* spp., $n = 274$ for *Bolinopsis* spp., $n = 200$ for *Bolinopsis* spp. size frequencies). The angle of orientation of the mouth (an indicator of general swimming direction) was measured using ImageJ v1.44p (Rasband, 1997–2012) by bisecting the imaged specimen from aboral to oral end. The software recorded the orientation angle and length of each specimen. Differences in size distributions of *Bolinopsis* spp. among days were assessed using one-sided Kolmogorov–Smirnov tests. For sampling the highly abundant copepods and appendicularians ($<$ 5 mm in size), 1/6th of a frame was subsampled on one profile from each transect (10 profiles per day) and 1 out of every 20 frames was examined, generating $\sim$2 samples per m of depth on each profile. This subsampling procedure was sufficient because there were typically several copepods and appendicularians in each image.

Because diatom aggregates (also known as 'flocculations' or 'flocs'; Alldredge *et al.*, 2002) were overwhelmingly the most common specimens in the images, we could use automated particle analysis available in ImageJ (Rasband, 1997–2012, 'Particle Analyzer') to calculate the particle size and shape features from one profile through a thin layer on 5 July. First, the images were thresholded (converted to black and white pixels) and particles >250 pixels in size were counted and sized, which effectively removed all of the copepods and appendicularians. ImageJ's 'Particle Analyzer' measured the major and minor axes of an ellipse fit to each particle, and the information from the maximum sized particle per frame was extracted. Since most of the diatom flocs were oblong in shape, the minor axis was used as a proxy for diameter. The ratio of the major to minor axis was used as a shape descriptor (lower values mean the particle is round and higher values more oblong). The values in pixels were converted to mm based on a known 13-cm field of view. Thin layer particles from 28 June were not measured because flocs were so dense that the individual particles could not be distinguished for analysis.

Data processing and generalized linear mixed models

Physical and biological data were merged to yield to precise environmental values (temperature, salinity, depth and chlorophyll-*a* fluorescence) for each gelatinous organisms found in the images. To obtain the average vertical distributions, all 30 profiles from each day were used, and the volume sampled in each 1 m depth bin was calculated based on the amount of time ISIIS spent in that depth bin. Counts of copepods and appendicularians were converted to concentrations by calculating the volume of water sampled in 1/6th of an ISIIS image and multiplying. Data analysis and visualization were performed in R (v2.15.2) (R Core Team, 2012) using the packages 'plyr' (Wickham, 2011) and 'ggplot2', respectively (Wickham, 2009).

Physical and biological data were processed to quantify the average environmental values and the total count of each gelatinous taxon for each m^3 of water sampled with ISIIS. This was accomplished by binning gelatinous organism data by the time it took to sample 1 m^3 of water (7.7 s) to yield ind. m^{-3} for each taxon; only the five most abundant taxa [*Pleurobrachia* spp., *Bolinopsis* spp. (small and large size classes), *Eutonina indicans*, *Muggiaea* spp. and *Sphaeronectes* spp.] were binned. Then, using the average timestamp within each gelatinous organism bin, each count per m^3 was matched to the nearest timestamps of chlorophyll-*a* fluorescence, temperature, salinity and depth. Depths and the thin layer analysis (discussed previously) were used to create thin layer categorical variables: each m^3 was characterized as being 'above a thin layer', 'within a thin layer', 'below a thin layer', or 'thin layer absent from the profile.'

Generalized linear mixed models (GLMMs) with log link function were implemented to determine the influence of sampling date, depth, fine-scale chlorophyll-*a* fluorescence and thin layer categorical variables (no thin layer, above, below and within the thin layer) on the number of gelatinous organisms per m^3. Although many ecological processes are expected to be nonlinear, preliminary plots showed some linear trends with respect to several explanatory variables. Also, the use of a linear model allowed for more intuitive interpretation of coefficients (similar interpretation as standard least squares modeling). Due to the collinearity of depth and temperature, temperature was dropped from the model and salinity was removed because there was little change along each profile. Models were fitted in R (v2.15.2) (R Core Team, 2012) with the package 'lme4' (Bates *et al.*, 2012) using the Laplace approximation, and the significance of model coefficients was assessed using Wald z tests. Interaction terms were not used because they can obscure the effects of the individual predictor variables (Gotelli and Ellison, 2004), and preliminary analyses produced no indication of strong interactions.

GLMM is an approach to generalized linear modeling that allows for a correlation structure to be incorporated into a model by differentiating between fixed and random effects. For this study, the spacing of organism counts was on the scale of meters; therefore, there was the potential for adjacent observations to be correlated (violation of independence) within a sampling profile (Zuur *et al.*, 2009). This correlation structure was accounted for by including the profile number as a random effect in the model. The model output produces coefficients that are proportional to the effect of a 1 unit increase of the variable on the expected concentrations of the organisms. Therefore, a positive coefficient indicates that the response variable (organism concentration) will increase in proportion to the value of that coefficient. GLMMs allow for modeling non-normal distributions (e.g. Poisson, binomial, etc.), and the use of random effects which essentially enables the user to parse out clusters of data that may contain autocorrelation (Bolker *et al.*, 2009). Correlation of residuals that was present when performing ordinary generalized linear modeling was eliminated through the use of a random profile effect.

Indices of patchiness and spatial overlap

While the random effects within the GLMM accounted for autocorrelation within a profile, a more intuitive

measure of patchiness over the entire sampling area was obtained using the scale independent Lloyd's index of patchiness (Lloyd, 1967).

$$\text{Patchiness} = 1 + \left(\frac{\sigma^2 - m}{m^2}\right) \quad (1)$$

where σ^2 is the sample variance and m the sample mean. A random distribution was assumed to follow the properties of the Poisson distribution, having equivalent means and variances, and would therefore have a patchiness index of 1. Indices >1 indicated aggregation of organisms. Lloyd's patchiness was applied for each day of sampling across all 1 m^3 sample bins.

To investigate the degree of spatial overlap of copepods and appendicularians with gelatinous predators, a spatial overlap index (O) was used (Williamson and Stoeckel, 1990):

$$O = \frac{\sum_{z=1}^{m} (N_z \times n_z)m}{\sum_{z=1}^{m} (N_z) \times \sum_{z=1}^{m} (n_z)} \quad (2)$$

where z represents the depth strata and m the number of depth strata sampled. N_z and n_z correspond to the concentration of copepods or appendicularians and the concentration of gelatinous zooplankton, respectively. If the overlap index is >1, this indicates spatial overlap of taxa. An index <1 indicates spatial separation. The index was calculated for each profile measured for copepods and appendicularians. To give an adequate number of samples per strata (>10), data were pooled into 3 m depth strata, and all samples taken <15 m were discarded because depth was variable among profiles.

RESULTS

Water column properties and thin layers

The study period (28 June to 7 July 2010) began after ~14 days of generally consistent upwelling favorable winds (Fig. 2a). However, a small relaxation event on 28 June and brief relaxation events shortly after likely led to a breakdown in thermal stratification in the study area by 30 June (Fig. 2a and b). Although upwelling (northwesterly) winds became consistent after 30 June, persistent, strong stratification did not occur again until 5 July. The winds on 5 July weakened and changed direction, but stratification did not decrease until the final day of sampling (7 July) when the winds had been calm for 2–3 days. 7 July was marked by lower overall chlorophyll fluorescence (a mean chlorophyll-*a* maximum of 1.004 V) and reduced thermal stratification. Salinity was fairly constant throughout the study (Δ0.06), but the autonomous profiler showed a distinct small drop in salinity just prior to the 2 July sampling date (Δ 0.03), potentially indicating the influx of California current water (J.P. Ryan, Monterey, pers. comm.). However, temperature/salinity diagrams from a concurrent study (Woodson *et al.*, in revision) demonstrated that offshore influx of water was minimal.

Thin layers were present on all days of sampling with the exception of 30 June, which was the only sampling performed at night. Thin layers were most common on 28 June and 5 July (thin layers observed on 47 and 87% of profiles with thin layers, respectively), which were also the days with higher chlorophyll-*a* maxima and strong thermocline and oxycline (Table I, Fig. 2b). *Pseudo-nitzschia* spp. was the dominant phytoplankter on all sampling days with some temporal variation in concentration (see Timmerman, 2012).

Automated particle counting revealed changes in the fine-scale structure of diatom flocs above, within and below a thin layer. Above the layer, particles were few in number but increased in concentration and size with depth (Fig. 3a). The higher major-to-minor axis ratio indicates the particles above the layer were oblong in shape and likely sinking (Fig. 3b). Within the high chlorophyll-*a* thin layer, flocs were numerous, large in size and relatively round (Fig. 3a and b). Below the layer, flocs were few in number but highly variable in size and shape.

Copepod and appendicularian abundances and vertical distributions

Copepods and appendicularians displayed strong temporal variability in both their overall abundances and vertical distributions. The mean copepod concentration was highest on days when thin layers were present, but the vertical distributions indicate that they did not aggregate within zones of high chlorophyll-*a* fluorescence (Table I, Fig. 4). The mean appendicularian concentration was highest on the last day of sampling (7 July). Lloyd's index of patchiness was consistently >1 for both groups on all days, indicating that there was aggregation (Table I).

The GLMMs revealed differences between the vertical distributions of appendicularians and copepods. When a thin layer was present in a profile, appendicularians were more abundant in all zones of the water column, while the copepod concentrations were not influenced by the presence of thin layers (Table II). The two groups had opposing responses to chlorophyll-*a* fluorescence; copepods, although not influenced by thickness of the chlorophyll-*a* maximum, generally tended to aggregate outside of zones of high chlorophyll-*a* and appendicularians were slightly more common when chlorophyll-*a* was higher (Table II). The model results are supported by 1 m bin averaged concentrations (Fig. 4), where copepods displayed a bimodal distribution with peak concentrations

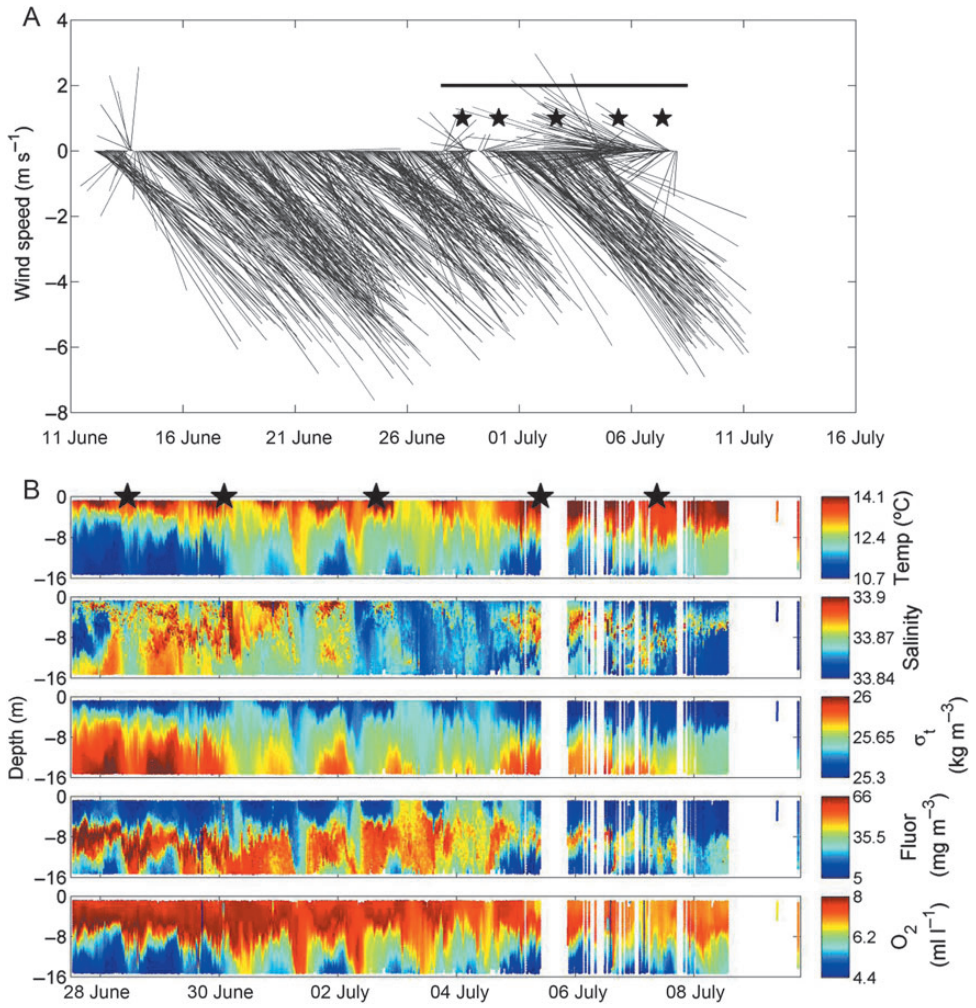

Fig. 2. (**A**) Prevailing wind speed and direction between 11 June 2010 and 8 July 2010 from a nearby NDBC station 46042. Winds with a significant northerly component (negative y value) are 'upwelling' winds. Black stars denote the times when sampling with ISIIS. Black horizontal line shows the time range when the SeaHorse profiler was in use. (**B**) SeaHorse profiler data showing the water column properties throughout the study period. Thin fluorescent layers (most common on 28 June and 5 July) are correlated with high thermal stratification. Gaps in SeaHorse data were due to technical difficulties with the instrument.

outside the zones of high chlorophyll-*a* fluorescence, whereas appendicularians showed a weak increase with depth and near zones of higher chlorophyll-*a*. The spatial overlap index showed that appendicularians consistently had more fine-scale spatial overlap with gelatinous zooplankton than did copepods, with an exception being the one night sampling period when the overlap indices were approximately equal (30 June, Fig. 5).

Gelatinous zooplankton abundance and vertical distribution

A total of 35 208 gelatinous animals were identified in the ISIIS profiles. Five species groups were most common, including the ctenophores *Pleurobrachia* spp. and *Bolinopsis* spp., *E. indicans* and the siphonophores *Muggiaea* spp. and *Sphaeronectes* spp. (Fig. 6). Several other species were also encountered in the images, including rare taxa such as *Sarsia tubulosa*, hydromedusae from the family Pandeidae, anthomedusae from the family Moerisiidae and the scyphomedusa *C. fuscescens. Bolinopsis* spp. was divided into two size classes because initially many small ctenophores without tentacles were extracted from the images, but it was later determined that almost all (>99%) of these ctenophores were juvenile *Bolinopsis* spp.

Overall abundances and the vertical distributions of the five most common gelatinous taxa (Fig. 6) changed dramatically throughout the study period. On 28 June abundances were low, but there were distinct vertical patterns with *Pleurobrachia* spp. most abundant near the surface, all taxa relatively common near the chlorophyll-*a*

*Table I: Statistics of chlorophyll-*a *aggregation on various sampling days for profiles examined for gelatinous zooplankton (*n = *15 for July 5,* n = *30 for all other days), primary consumer (copepods and appendicularians) abundances, and aggregation statistics*

Date	28 June	30 June	2 July	5 July	7 July
Mean chlorophyll max (V) (SE)	2.163 (0.086)	1.306 (0.031)	1.504 (0.027)	1.610 (0.022)	1.004 (0.023)
Mean depth of chlorophyll max (m) (SE)	8.620 (0.291)	12.249 (0.354)	6.189 (0.310)	7.031 (0.162)	9.626 (0.381)
Profiles with thin layers	14	0	7	13	6
Percent of profiles with thin layers	47	0	23	87	20
Mean copepod concentration (ind. m^{-3}) (SE)	5301 (97.54)	5067 (81.66)	4282 (71.78)	8453 (264.37)	4644 (90.55)
Maximum copepod concentration (ind. m^{-3})	20 421	23 612	29 994	37 014	22 336
Copepods Lloyd's patchiness	1.23	1.26	1.38	1.53	1.42
Mean appendicularian concentration (ind. m^{-3}) (SE)	5870 (79.81)	2176 (38.45)	5474 (104.01)	4835 (126.16)	10 610 (102.47)
Maximum appendicularian concentration (ind. m^{-3})	17 868	10 848	22 974	19 145	25 527
Appendicularian Lloyd's patchiness	1.08	1.17	1.56	1.29	1.08

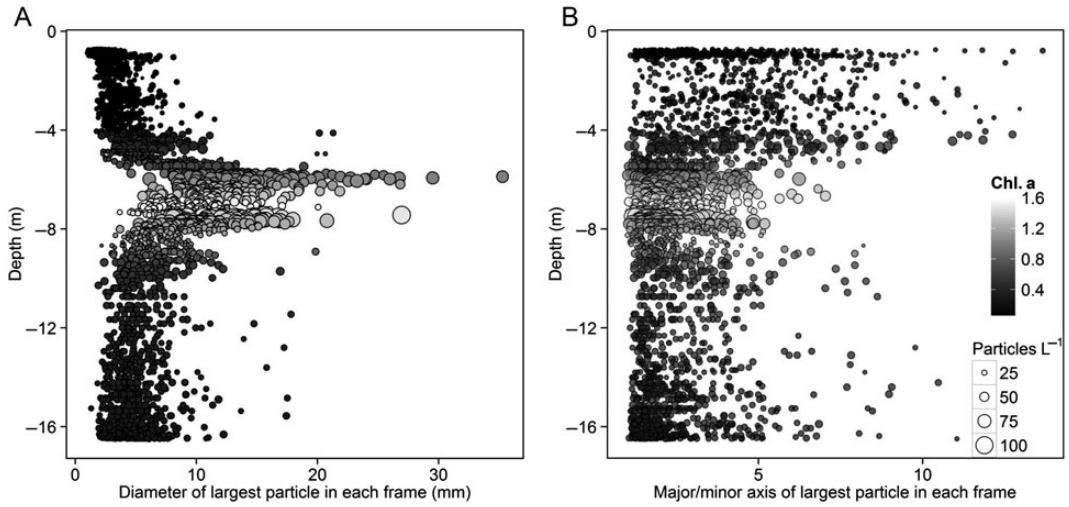

Fig. 3. (**A**) An average minor (horizontal) axis of particles in each ISIIS frame gives an estimate of diatom floc size. Size of each point is proportional to the number of flocs in each ISIIS image. Color corresponds to chlorophyll-*a* fluorescence (V) (**B**) Ratio of major (vertical) to minor (horizontal) axis. Higher ratios mean the particles are oblong and likely sinking at a fast rate. Lower ratios indicate a more round particle that is likely sinking slowly.

fluorescence maximum, and *E. indicans* was more common at depth (Fig. 7). By 2 July, *E. indicans* and small *Bolinopsis* spp. were the most abundant, with *E. indicans* highly patchy and aggregated at depth (Table III, Fig. 7). The fifth of July was marked by a significant increase in *Bolinopsis* spp. ctenophores (an instantaneous exponential growth rate of 0.54 between 2 July and 5 July—assuming no advection), as well as peak abundances for the other two ctenophore groups (Fig. 7). The two siphonophore species (*Muggiaea* spp. and *Sphaeronectes* spp.) also reached relatively high abundances on 5 July and remained common on 7 July (Fig. 7). The concentration of all six common gelatinous organism taxa combined tended to increase in relation to depth on all days of sampling (except for 28 June), regardless of the prevalence of thin layers (Table IV, Fig. 7).

GLMMs with a random profile effect accounting for small-scale autocorrelation revealed different influences of biological and physical parameters among the gelatinous taxa. Model coefficients showed taxa were more likely to be present and in higher concentrations (counts) at greater depths, and they were highly aggregated in their distributions (Tables III and IV). *Eutonina indicans* was most abundant at greater depths and had the most aggregated distribution, with extremely high concentrations on 2 July (a maximum concentration of 251 ind. m^{-3}). The concentrations of *Bolinopsis* spp. were positively influenced by higher chlorophyll-*a* (Table IV), while the concentrations of other taxa were either slightly elevated (*Pleurobrachia* spp.) or unaffected. Only *Bolinopsis* spp. was more abundant within thin layers, but the concentrations of several taxa were higher below thin layers (Table IV).

Measurements of *in situ* orientation and daily size structure were made as indicators of behavioral

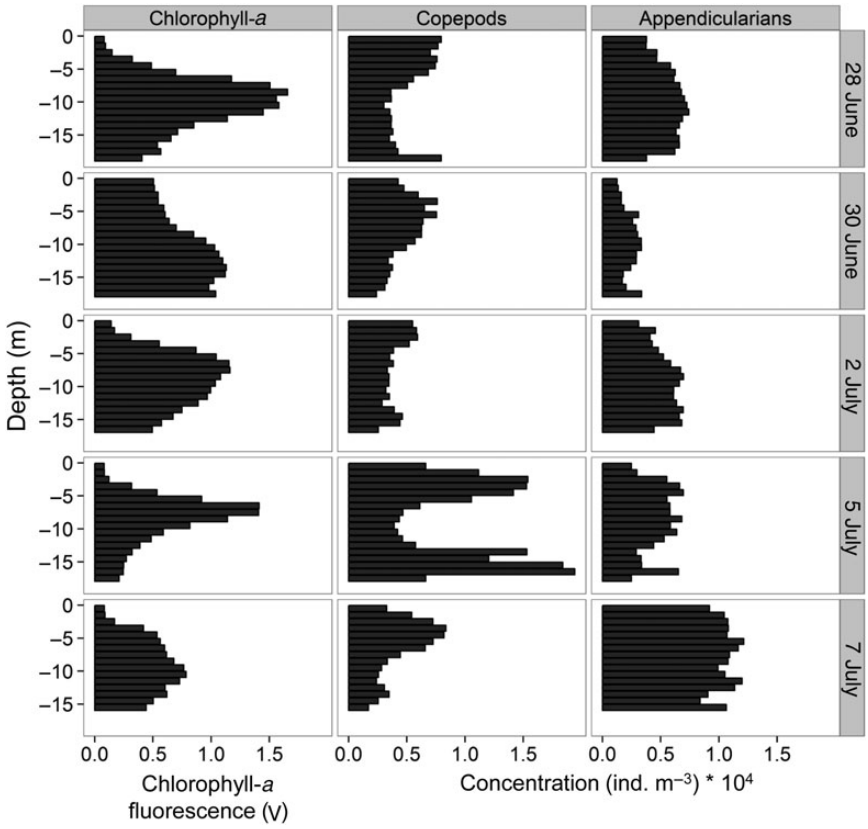

Fig. 4. An average concentration of chlorophyll-*a* fluorescence (V) and zooplankton (ind. $m^{-3} * 10^4$) in 1 m depth bins on each of the five ISIIS sampling days.

Table II: Fixed effects for Poisson GLMMs for copepods and appendicularians

	Copepods		Appendicularians	
Model parameters	Coefficient	*P*	Coefficient	*P*
Date 30 June	−0.0303	ns	−0.7718	**
Date 2 July	−0.4422	*	−0.4557	*
Date 5 July	0.2197	ns	−0.3453	ns
Date 7 July	−0.3388	ns	0.6776	**
Depth	−0.0020	ns	0.0073	***
Fluorometry	−0.5006	***	0.1858	***
Above layer	0.2708	ns	0.3737	*
Below layer	−0.2777	ns	0.4160	*
Within layer	0.0519	ns	0.3708	*

Profile number was treated as a random effect to account for spatial autocorrelation between nearby samples. Model coefficients and significance levels are shown. Significance was assessed using Wald *z* tests.
Model formula:
Count ~ profile number + date + depth + fluorometry + thin layer category.
P value significance codes are as follows: $P > 0.05$ = ns, $0.01 < *P < 0.05$, $0.001 < **P < 0.01$ and $***P < 0.001$.

characteristics and growth, respectively, of ctenophores within the bay. The *in situ* orientation of *Bolinopsis* spp. indicated that they were typically cruising the water column vertically, with oral end (and lobes) pointed down, perpendicular to the thin layers and/or chlorophyll maximum (Fig. 8a), while *Pleurobrachia* spp. had less consistent orientation (Fig. 8b), though with a predominately vertical (oral end up) orientation. The length/frequency histograms of a subsample *Bolinopsis* spp. for each day show a significant increase in size on subsequent sampling days (one-sided Kolmogorov–Smirnov tests, Fig. 9). A linear growth rate extracted from the modal size (rounded to nearest 0.2 mm) was 0.45 mm day^{-1}, assuming ctenophores are being sampled from the same population.

DISCUSSION

Fine-scale distribution data obtained by ISIIS showed strong vertical heterogeneity in three separate trophic levels including phytoplankton, primary consumers and gelatinous zooplankton, with >2 orders of magnitude difference between surface and 15 m depth concentrations of the gelatinous zooplankton. Water column stratification likely caused passive accumulation of non-motile diatoms *Pseudo-nitzschia* spp., the most abundant

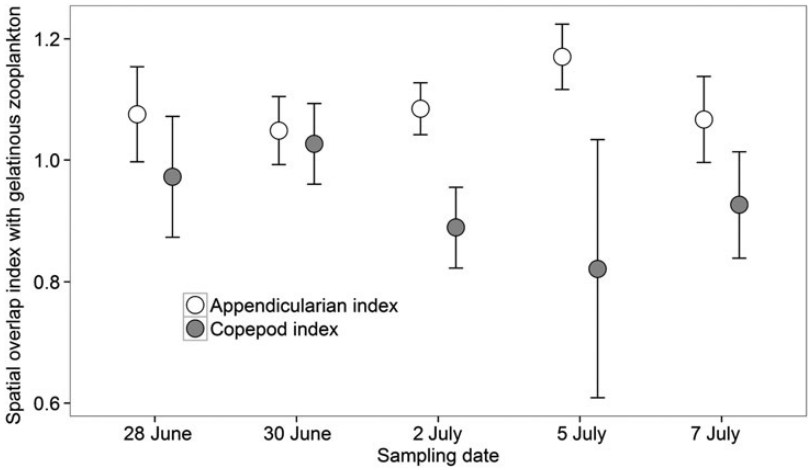

Fig. 5. A spatial overlap index between primary consumers (copepods and appendicularians) and the total gelatinous zooplankton abundance in 1 m^3 surrounding the sample. Indices >1 indicate spatial overlap and <1 spatial separation. Error bars represent 1.96 times the standard error of the index.

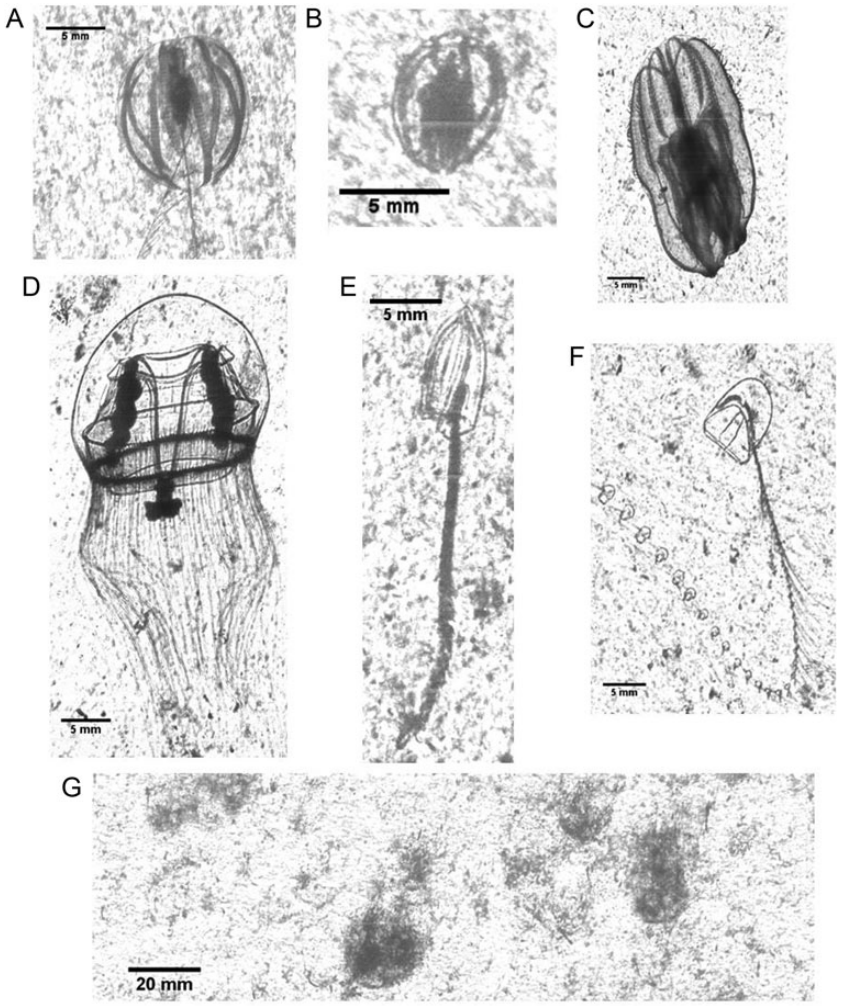

Fig. 6. Specimens imaged by ISIIS (**A**) *Pleurobrachia* spp. (**B**) small *Bolinopsis* spp. (**C**) large *Bolinopsis* spp. (**D**) *E. indicans* (**E**) *Muggiaea* spp. and (**F**) *Sphaeronectes* spp. – Notice the cormidia bearing developing sexual medusoids. (**G**) *Pseudo-nitzschia* spp. diatom flocs within a thin layer from July 5. Scale bars are 5 mm for A–F, 20 mm for G.

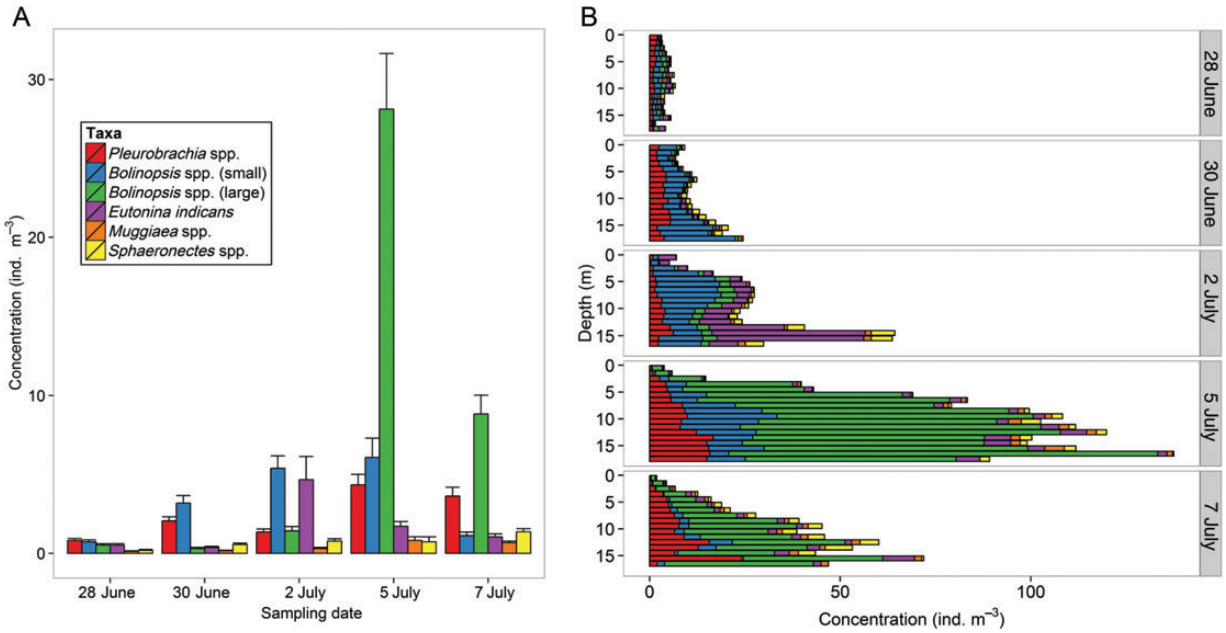

Fig. 7. (**A**) Water column average concentration of different gelatinous zooplankton by day of sampling. Each profile through the water column was considered a sample ($n = 30$ per sampling day, $n = 15$ on July 5) and error bars represent 1.96 * standard error. (**B**) Vertical distribution (ind. m^{-3}) of gelatinous zooplankton in 1 m vertical depth bins. Bars are stacked (non-overlapping).

phytoplankter in the study area. Thin layers were most common on days when the water column was thermally stratified (28 June and 5 July), and GLMMs fit to organism counts per m^3 showed differing patterns between zooplankton taxa in relation to thin layers, chlorophyll-*a* fluorescence and depth.

Diatom dominated thin layers and primary consumers

The temporal persistence was the primary difference between the thin layers on 28 June and 5 July, and the lack of motility of the dominant phytoplankter had a large influence on the assumed mechanism of formation. The layer on 28 June could have been present for up to 10 days due to consistent, strong upwelling winds before the study began. Because of these winds, the upwelling shadow had likely retained water within the bay for up to 14 days, with *Pseudo-nitzschia* spp. located at the base of the pycnocline. These non-motile diatoms have been previously shown to accumulate at density interfaces (MacIntyre *et al.*, 1995; Cheriton *et al.*, 2009), and high thermal stratification likely kept *Pseudo-nitzschia* spp. in a thin layer near the pycnocline on 28 June, but the diatoms were possibly actively growing above the layer where oxygen was relatively high (ΔO_2 2.1 mL L^{-1}). The thin layer on 5 July was also driven by thermal stratification but was newly formed and had higher abundances of smaller phytoplankton (Timmerman, 2012). Size/shape descriptors obtained from thin layer particles on 5 July is consistent with the concept of diatoms flocculating and settling at a thermocline because within the thin layer, particles were larger, rounder and more abundant. In other cases, thin layers are composed of motile species of phytoplankton, such as the dinoflagellate *Akashiwo sanguinea* (Rines *et al.*, 2010). In these cases, behavioral cues, rather than sinking and settlement in diatoms, may play a more important role.

Although there was a non-uniform distribution of fluorescence on all days, the primary diatom consumers, copepods, were not found in high concentrations within thin layers. A GLMM showed a negative influence of chlorophyll-*a* on copepod concentrations. Copepods were typically most abundant near the surface, where chlorophyll-*a* fluorescence was low, and also sometimes aggregated below thin layers (5 July). Copepod aggregations outside of chlorophyll-*a* maxima have been documented previously using water samples and acoustic methods (Herman, 1983; Nielsen *et al.*, 1990; Jaffe *et al.*, 1998; Alldredge *et al.*, 2002; Holliday *et al.*, 2003, 2010; McManus *et al.*, 2005). The thin layers on 28 July were deeper, more intense in their chlorophyll-*a* fluorescence and thicker than the layers on 5 July (Table I), which may have affected the vertical distributions of copepods. *Pseudo-nitzschia* spp. in our study was producing the toxin domoic acid, which has been demonstrated to inhibit grazing in krill (Bargu *et al.*, 2006; Timmerman *et al.*, in press), and it may have a similar effect on other grazers, such as copepods, thereby increasing the persistence of a bloom. Although domoic acid has been shown

Table III: Summary statistics for gelatinous zooplankton abundances

Species	Date	Mean concentration (inds m^{-3})	Standard error	Maximum concentration (inds m^{-3})	Lloyd's patchiness	Proportion of m^3 sampled with >1 gelatinous organisms per m^3
Pleurobrachia spp.	28 June	0.8175	0.1002	9	2.7515	0.4079
	30 June	2.0591	0.2762	20	2.5039	0.6517
	2 July	1.3516	0.1991	16	2.9293	0.4726
	5 July	4.3396	0.4989	37	2.3829	0.7090
	7 July	3.6206	0.7682	44	3.9983	0.5832
Small *Bolinopsis* spp.	28 June	0.7299	0.1050	13	3.8088	0.3274
	30 June	3.1833	0.4730	54	3.5806	0.7088
	2 July	5.3894	0.9034	68	3.7191	0.6144
	5 July	6.0784	1.1129	72	3.6205	0.5896
	7 July	1.1194	0.2392	28	5.7178	0.2955
Large *Bolinopsis* spp.	28 June	0.5188	0.06850	8	3.3044	0.2880
	30 June	0.3014	0.09649	10	7.5519	0.1690
	2 July	1.4234	0.3218	35	5.5256	0.3932
	5 July	28.1157	2.4464	144	2.0584	0.8022
	7 July	8.8258	1.4861	75	3.3481	0.6634
E. indicans	28 June	0.5206	0.07849	10	3.2553	0.3077
	30 June	0.3747	0.05064	5	2.0379	0.2668
	2 July	4.6711	1.4786	251	14.4520	0.6522
	5 July	1.7201	0.2696	14	2.3148	0.5858
	7 July	1.0391	0.2672	18	4.6522	0.3601
Muggiaea spp.	28 June	0.1270	0.03056	3	3.3450	0.1020
	30 June	0.1568	0.02687	2	2.1685	0.1303
	2 July	0.3081	0.05988	5	3.5151	0.1966
	5 July	0.8209	0.2435	15	5.3587	0.3396
	7 July	0.6732	0.06055	7	2.0605	0.3933
Sphaeronectes spp.	28 June	0.1825	0.05863	7	10.6655	0.1002
	30 June	0.5601	0.05812	9	2.3047	0.3483
	2 July	0.7713	0.1240	11	3.5151	0.2665
	5 July	0.7351	0.2733	33	5.3587	0.2575
	7 July	1.3659	0.1373	17	2.0605	0.4462

Table IV: Fixed effects from GLMMs for the six most common gelatinous taxa

	Pleurobrachia spp.		*Bolinopsis* spp. (small)		*Bolinopsis* spp. (large)		*E. indicans*		*Muggiaea* spp.		*Sphaeronectes* spp.	
Model parameters	Coefficient	*P*	Coefficient	*P*	Coefficient	*P*	Coefficient	*P*	Coefficient	*P*	Coefficient	*P*
30 June	1.0040	***	1.6893	***	−0.3890	ns	−0.1937	ns	0.4787	ns	1.7076	***
2 July	0.5112	*	1.9158	***	1.0617	***	1.6779	***	0.9152	**	1.8341	***
5 July	1.8751	***	2.5120	***	4.5574	***	1.2858	***	1.9323	***	1.8660	***
7 July	1.3433	***	0.0226	ns	3.6138	***	0.4729	ns	2.2906	***	2.9988	***
Depth	0.0816	***	0.0256	***	0.0902	***	0.1165	***	0.0855	***	0.1926	***
Chl-*a*	0.2125	***	0.8031	***	0.8783	***	−0.0062	ns	0.3243	**	0.1995	ns
Above layer	−0.0031	ns	−0.6358	*	0.2510	ns	−0.1618	ns	0.0306	ns	−0.9434	**
Below layer	0.2975	ns	0.1850	ns	0.8286	***	0.6243	*	0.5855	*	0.2359	ns
Within layer	0.3037	ns	0.4358	*	0.7570	**	0.1522	ns	0.3661	ns	0.2080	ns

Models use organism counts per m^3 as a response variable to sampling date, depth, chlorophyll-*a* fluorescence (chl-*a*) and thin layer categorical variables. Sampling date coefficients are fit relative to the first date of sampling (28 June) and thin layer variables are fit relative to the 'no thin layer present' category. The profile number was used as a random effect to account for the correlation structure within a profile.

experimentally to have no effect on feeding and growth in copepods (Lincoln *et al.*, 2001), copepods could still preferentially occupy waters that contain fewer toxins. There were indications of bimodal vertical distributions in copepods on all sampling days, with the exception of 30 June, which was the only night sampling period and had a deeper and diffuse chlorophyll-*a* profile (no thin layers). Even on the night of 30 June, the copepods were not observed to aggregate inside the zone of high chlorophyll-*a* fluorescence. Diatoms within thin layers tended to form dense flocs; it is possible that on the edges of thin layers, copepods may find diatoms in a more 'palatable' form, or they utilize short excursions into the layers to feed (Bochdansky and Bollens, 2004).

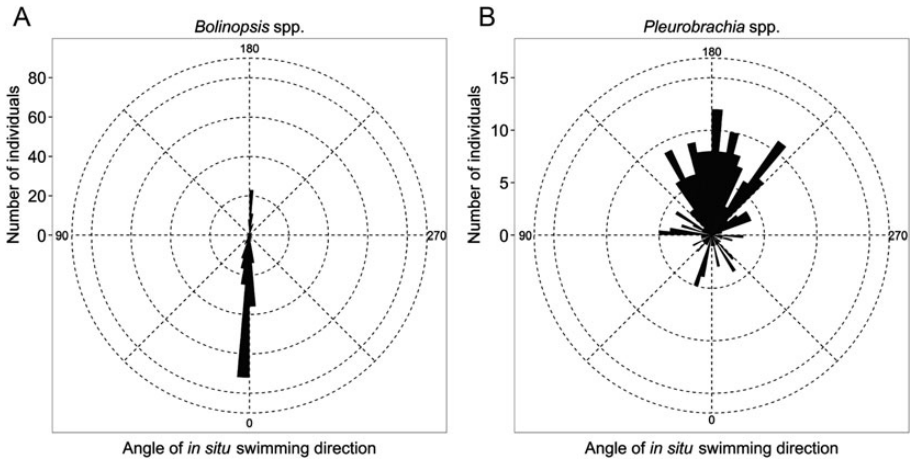

Fig. 8. Polar histograms showing the angle of *in situ* orientation (and swimming) of the oral end for subsets of (**A**) *Bolinopsis* spp. ($n = 274$) and (**B**) *Pleurobrachia* spp. ($n = 225$) ctenophores. 180° is towards the surface and 0° towards the benthos. Much more consistent vertical orientation is displayed in *Bolinopsis* spp.

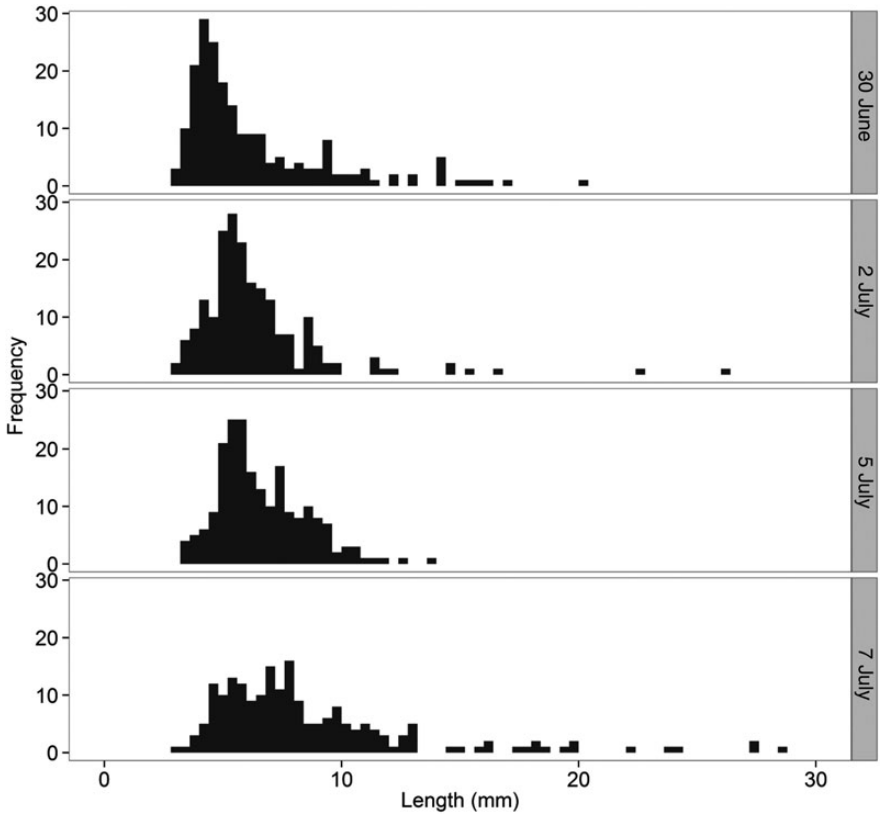

Fig. 9. The length/frequency histograms of *Bolinopsis* spp. (small and large size classes pooled) from 4 days of sampling. One-sided Kolmogorov–Smirnov tests revealed significant right shifts in size distributions between sampling days.

Vertical distributions of zooplankton predators and prey

Although depth was not a significant predictor variable in the GLMM, copepod peak abundances tended to occur within the shallowest 5 m of the water column, where chlorophyll-*a* levels and gelatinous predator abundances were low. For every profile, the lowest measured values of chlorophyll-*a* fluorescence were found near the surface, which tended to be dominated by copepods. In contrast, *Bolinopsis* spp. ctenophores were particularly

abundant within and below thin layers (and at greater depths in general). The spatial overlap index between copepods and gelatinous zooplankton was <1 indicating spatial separation, which is consistent with the concept of predation avoidance. Thus, it is possible that the copepods in Monterey Bay use the surface as a predation refuge and make short bouts into the deeper predator abundant waters to feed. Such a strategy would allow the copepods to minimize their predation risk while still being able to feed and is consistent with the 'predation avoidance' hypothesis of vertical migration (Zaret and Suffern, 1976) supported by several copepod behavior studies (e.g. Neill, 1990; Dawidowicz *et al.*, 1990). Field evidence has also shown that copepods vertically migrate depending on their body condition, only risking vertical migration into predator dense zones if their oil sac is depleted (Hays *et al.*, 2001). In addition, copepods grow faster and reproduce more in water with higher temperatures (Bonnet *et al.*, 2009), so occupying the surface waters could have multiple positive effects on the population.

Appendicularians had a positive relationship with depth and chlorophyll-*a* fluorescence, potentially due to less predation pressure (when compared with copepods). Of the species in this study, appendicularians are only known to be preyed upon by *E. indicans* (Wrobel and Mills, 1998) and so when compared with copepods, the predation risk of occupying thin layers is likely substantially less. Food availability, therefore, may be the primary influence on their distributions. Appendicularians are capable of feeding on a wide range of phytoplankton sizes, including pico and nanoplankton, which are abundant in nutrient-poor offshore waters of Monterey Bay (Ryan *et al.*, 2009). The positive association of appendicularians within and around thin layers may indicate that properties associated with thin layer formation (i.e., water column stability and concentrated sources of phytoplankton) are favorable to appendicularian population growth.

Gelatinous zooplankton (predators of copepods and appendicularians) were more abundant at greater depths on all sampling days, regardless of the stratification regime present, and this pattern may exist due to a combination of three factors: negative effects of copepods on gelatinous zooplankton reproduction, contact predator advantages and avoidance of visual predators. Copepods demonstrated less spatial overlap with gelatinous zooplankton compared with appendicularians. Although the ctenophores in this study tend to consume copepods (Reeve *et al.*, 1978; Greene *et al.*, 1986), they have a complex relationship with these prey. Studies of ctenophores using enclosures have shown that high concentrations of copepods can severely reduce the survival of larval ctenophores (Stanlaw *et al.*, 1981). Therefore, above certain prey concentrations, ctenophores may become less effective predators due to inhibited reproductive success. Another potential benefit to gelatinous zooplankton occupying deeper waters is that ambient light levels influence the competitive advantage of contact versus visual predation. An experiment by Sørnes and Aksnes (2004) demonstrated that *Bolinopsis* spp. feeding reaches an asymptote at high prey concentrations, and when light levels are lower, tactile predation becomes more advantageous than visual predation. While irradiance was not measured in this study, a previous study in the same area found that several wavelengths of light experience $\sim$100-fold reductions below a thin layer of *Pseudo-nitzschia* spp. in Monterey Bay (Sullivan *et al.*, 2010). Attenuation of light was almost certain to increase in the region of the pycnocline during our study, with diatom flocs larger and more abundant within thin layers. The thin layer of *Pseudo-nitzschia* spp., therefore, could set up microhabitats in which visual predation on copepods dominates above the thin layer (perhaps by planktivorous fishes), while tactile predation is more advantageous below. Jellies also have many visual predators (Oviatt and Kremer, 1977; Link and Ford, 2006) that can likely be avoided by occupying zones of lower light levels. Therefore, surface waters may be zones of the water column where jellies are less fecund, inferior predators (outcompeted by visual predators) and exposed to higher visual predation by their own suite of predators.

Gelatinous zooplankton and diatom thin layers

The idea of gelationous organisms aggregating at density discontinuities is not new (Arai, 1976; Mills, 1984; Graham *et al.*, 2001; Jacobsen and Norrbin, 2009), but the results of this study demonstrate that only one species (*Bolinopsis* spp.) tends to aggregate within thin layers and vertical density discontinuities. This may indicate that the vertical swimming of *Bolinopsis* spp. results in increased probability of thin layer encounter, as species with a horizontal or random swimming pattern would not be expected to encounter vertical density discontinuities as frequently as a vertical swimmer. Indeed, *Bolinopsis* spp. behavior in this study as well as others (Reeve *et al.*, 1978; Toyokawa *et al.*, 2003) suggests precise vertical orientation in this species is common. In contrast, *Pleurobrachia* spp. displayed a more variable swimming pattern, perhaps related its behavior of swimming straight or in an arc to spread its tentacles for feeding (Reeve *et al.*, 1978). When feeding, *Pleurobrachia* spp. drifts passively (Purcell, 1991) and so it could be subjected to microturbulence causing variable orientation.

Of all the gelatinous zooplankton examined, only *Bolinopsis* spp. was found in significantly higher

abundance within thin layers. This raises the question why a zooplankton predator would occupy a thin layer of phytoplankton, especially when its prey items are abundant above and below the layer. The ISIIS images displayed precise vertical orientation behavior of *Bolinopsis* spp., which is known to cruise the water column vertically in pursuit of prey (Reeve *et al.*, 1978). Moving through a density interface (pycnocline) would cause the vertical cruising speed of the *Bolinopsis* spp. to be reduced (by physical mechanisms), thereby causing an accumulation of ctenophores where passively sinking *Pseudo-nitzschia* spp. tended to aggregate. In addition, while traces of diatoms have been found in the guts of *Bolinopsis* spp., they cannot maintain their size on these prey items alone, suggesting that diatom consumption may be a method to ward off starvation (Reeve, 1980). Indeed, carbon and nitrogen stable isotope analysis demonstrates *Bolinopsis* spp. occupies a relatively low trophic position in the food web (Toyokawa *et al.*, 2003). Alternatively, ctenophores may actively seek temperature discontinuities and slow their swimming speed within them. Based on mesocosm experiments, it is likely that these ctenophores are actively responding to the density discontinuities (Frost *et al.*, 2010), but further controlled studies on *Bolinopsis* spp. would be needed to distinguish between these passive and active aggregation mechanisms.

Gelatinous organism blooms

The gelatinous organism 'bloom', defined as a rapid increase in the population abundance (Graham *et al.*, 2001), of *Bolinopsis* spp. between 30 June and 5 July may have been due to retention of ctenophores within the bay coupled with extremely fast growth rates. In captivity, *Bolinopsis* spp. has been shown to be capable of growing over 10 mm per day, and initiates reproduction when it becomes fully lobate at a size of ∼10 mm (Greve, 1970). According to temperature/salinity diagrams, the bay waters were retained during our study (i.e. not replaced by offshore California current water; Woodson *et al.*, in revision) and so a bloom could have formed within the bay. Tidal ellipses occurred below the thermocline (Woodson *et al.*, in revision) that may have acted as a retention mechanism, keeping ctenophores within the bay. Thin layers are also known as zones of reduced flow (McManus *et al.*, 2005) and so *Bolinopsis* spp. occupying these zones within the thermocline could have increased retention, improving the chances of a bloom. When food and flow conditions are favorable, remarkable growth rates, combined with simultaneous hermaphroditism (capable of self-fertilization) and high fecundities (Baker and Reeve, 1974; Reeve *et al.*, 1978; Costello *et al.*, 2006) likely allow this species to form blooms. The reduction in *Bolinopsis* spp. abundance on 7 July may have been due to cannibalism, which is known to occur in a closely related species (*Mnemiopsis leidyi*) (Javidpour *et al.*, 2009); however, trends in abundance with depth on 7 July indicate that ctenophores were possibly aggregating within 5 m of the bottom, which we were unable to sample. The increase in the length of *Bolinopsis* spp. over time, low Lloyd's patchiness and the circulation patterns suggest the phenomenon observed on 5 July was a 'true bloom' and not just a congregation of gelatinous animals due to physical convergence (Graham *et al.*, 2001).

On the other hand, the high abundance of *E. indicans* on 2 July was likely an 'apparent bloom' because dense aggregations were present on only about three profiles in waters deeper than the 20 m isobath, causing Lloyd's patchiness to be extremely high (14.452, Table III). In addition, laboratory obtained size at age of *E. indicans* suggests the organisms we sampled were >50 days old (Rees, 1978), and therefore were likely advected into the area well before the study commenced.

Importance of behavior in thin layer trophic interactions

Zooplankton studies using high resolution instruments sometimes appear to show avoidance thin layers of diatoms. In a recent study by Talapatra *et al.* (Talapatra *et al.*, 2013), two vertical profiles with an imaging system showed thin layers of *Chaetoceros socialis* and high particle counts within the vicinity of the pycnocline. In the first ascent, the zooplankton were located outside several, but not all, of the particle concentration peaks. In the second ascent, the zooplankton appeared to avoid the layers with elevated particle concentration (Talapatra *et al.*, 2013). Other field studies demonstrate that trophic interactions can occur within thin layers on sub-hour time scales, and the grazers spend more time within thin layers when a higher fraction of water column phytoplankton is contained within the layers (Benoit-Bird *et al.*, 2010; Holliday *et al.*, 2010). The temporal resolution of sampling in our study may not have been adequate to capture these brief events often enough to yield a statistically significant overlap.

The primary fluorescent organisms in this study were *Pseudo-nitzschia* spp., which lack swimming ability, so if passive accumulation was occurring across all taxa, then all observed plankton would strongly overlap with the chlorophyll-*a* fluorescence activity. This was not the case. In fact, similarly sized copepods and appendicularians had very different vertical distributions, indicating that behavior is an important driver of vertical distributions of zooplankton in this system. The density discontinuities present near the chlorophyll maximum combined with consistent vertical swimming of *Bolinopsis* spp. may have

led to accumulation and spatial overlap with higher chlorophyll-*a* levels and thin layers. Surface waters containing low abundances of gelatinous predators may serve as a predation refuge for copepods, which tend to aggregate at the surface despite low amounts of chlorophyll-*a* fluorescence activity in this zone. Further studies on copepod condition in different portions of the water column would elucidate some of the drivers of the strong spatial offset we observed between copepods and chlorophyll-*a* fluorescence. Copepods must strike a balance between predation avoidance and feeding, and the increases in gelatinous organism abundance with depth show that there are trade-offs to venturing into zones of higher phytoplankton concentrations.

In situ imaging technology provided a unique glimpse at an often overlooked component of marine food webs, gelatinous zooplankton, and placed them into the context of thin layers, which are common features in coastal environments. Acoustic surveys have detected thin layers but, unlike optical systems, are biased towards plankton with either an exoskeleton or gas bladder. The results of this study demonstrated that zooplankton of similar size, whose distributions are thought to be driven by physical forcing, can have strong differences in their vertical distributions. Optical systems serve as an ideal platform to better understand behavioral tendencies of zooplankton through both high resolution sampling and *in situ* orientation information. These characteristics should be considered (in conjunction with the physical environment) for studies on the causes of vertical heterogeneity in coastal ecosystems.

ACKNOWLEDGEMENTS

We thank Dorothy Tang for helping greatly with the identification and enumeration of zooplankton in the ISIIS images. Jessica Luo provided assistance in the field. Thanks to John Walter for help with statistical modeling. Su Sponaugle and Peter Ortner's comments and edits greatly improved early versions of the manuscript. Claudia E. Mills and Philip R. Pugh verified some of the ctenophore and siphonophore identifications. We would like to give a special thanks to Jim Christmann, captain of the R/V Shana Rae for making the field work a success. Brock Woodson and Ross Timmerman assisted in setting up the SeaHorse profiler. Raphael Kudela provided laboratory space for analysis of phytoplankton samples. We would also like to thank the other members of the Lateral Mixing Project including Steven Monismith, Derek Fong, Ryan Moniz, Mark Stacey, Susan Willis, John Ryan and Olivia Cheriton for productive conversations and data sharing.

FUNDING

Funding was provided by an NSF RAPID grant to R.K. Cowen No. 1035047.

REFERENCES

Alldredge, A. L., Cowles, T. J., MacIntyre, S. *et al.* (2002) Occurrence and mechanisms of formation of a dramatic thin layer of marine snow in a shallow pacific fjord. *Mar. Ecol. Prog. Ser.*, **233**, 1–12.

Arai, M. N. (1976) Behavior of planktonic coelenterates in temperature and salinity discontinuity layers. In Mackie, G. O. (ed.), *Coelenterate Ecology and Behavior.* Plenum Press, New York, pp. 211–217.

Baker, L. D. and Reeve, M. R. (1974) Laboratory culture of the lobate ctenophore *Mnemiopsis mccradyi* with notes on feeding and fecundity. *Mar. Biol.*, **26**, 57–62.

Bargu, S., Lefebvre, K. and Silver, M. W. (2006) Effect of dissolved domoic acid on the grazing rate of krill *Euphausia pacifica*. *Mar. Ecol. Prog. Ser.*, **312**, 169–175.

Bates, D., Maechler, M. and Bolker, B. (2012) lme4: Linear mixed-effects models using S4 classes. R Packages Version 0.999999–0. http://CRAN.R-Project.org/package=lme4.

Benoit-Bird, K. J., Moline, M. A., Waluk, C. M. *et al.* (2010) Integrated measurements of acoustical and optical thin layers I: Vertical scales of association. *Cont. Shelf Res.*, **30**, 17–28.

Bochdansky, A. B. and Bollens, S. M. (2004) Relevant scales in zooplankton ecology: distribution, feeding, and reproduction of the copepod *Acartia hudsonica* in response to thin layers of the diatom skeletonema costatum. *Limnol. Oceanogr.*, **49**, 625–636.

Bolker, B. M., Brooks, M. E., Clark, C. J. *et al.* (2009) Generalized linear mixed models: a practical guide for ecology and evolution. *Trends Ecol. Evol.*, **24**, 127–135.

Bonnet, D., Harris, R. P., Yebra, L. *et al.* (2009) Temperature effects on *Calanus helgolandicus* (copepoda: Calanoida) development time and egg production. *J. Plankton Res.*, **31**, 31–44.

Breaker, L. C. and Broenkow, W. W. (1994) The circulation of Monterey Bay and related processes. *Oceanogr. Mar. Biol.*, **32**, 1–64.

Brierley, A. S., Boyer, D. C., Axelsen, B. E. *et al.* (2005) Towards the acoustic estimation of jellyfish abundance. *Mar. Ecol. Prog Ser.*, **295**, 105–111.

Cheriton, O. M., McManus, M. A., Stacey, M. T. *et al.* (2009) Physical and biological controls on the maintenance and dissipation of a thin phytoplankton layer. *Mar. Ecol. Prog. Ser.*, **378**, 55–69.

Costello, J. H., Sullivan, B. K., Gifford, D. J. *et al.* (2006) Seasonal refugia, shoreward thermal amplification, and metapopulation dynamics of the ctenophore *Mnemiopsis leidyi* in Narragansett Bay, Rhode Island. *Limnol. Oceanogr.*, **51**, 1819–1831.

Cowen, R. K. and Guigand, C. M. (2008) *In situ* ichthyoplankton imaging system (ISIIS): system design and preliminary results. *Limnol. Oceanogr. Methods*, **6**, 126–132.

Cowles, T. J. and Desiderio, R. A. (1993) Resolution of biological microstructure through in situ fluorescence emission spectra. *Oceanography*, **6**, 105–111.

Cowles, T. J., Desiderio, R. A. and Carr, M. E. (1998) Small-scale planktonic structure: persistence and trophic consequences. *Oceanography*, **11**, 4–9.

Dawidowicz, P., Pijanowska, J. and Ciechomski, K. (1990) Vertical migration of chaoborus larvae is induced by the presence of fish. *Limnol. Oceanogr.*, **35**, 1631–1637.

Dekshenieks, M. M., Donaghay, P. L., Sullivan, J. M. *et al.* (2001) Temporal and spatial occurrence of thin phytoplankton layers in relation to physical processes. *Mar. Ecol. Prog. Ser.*, **223**, 61–71.

Donaghay, P. L., Rines, H. M. and Sieburth, J. M. (1992) Simultaneous sampling of fine scale biological, chemical, and physical structure in stratified waters. *Arch. Hydrobiol. Beih.*, **36**, 97–108.

Frost, J. R., Jacoby, C. A. and Youngbluth, M. J. (2010) Behavior of *Nemopsis bachei* L. Agassiz, 1849 medusae in the presence of physical gradients and biological thin layers. *Hydrobiologia*, **645**, 97–111.

Gotelli, N. J. and Ellison, A. M. (2004) *A Primer of Ecological Statistics*. Sinauer Associates, Inc., Sunderland, MA, USA.

Graham, W. M. (1993) Spatio-temporal scale assessment of an 'upwelling shadow' in northern Monterey Bay, California. *Estuaries*, **16**, 83–91.

Graham, W. M. and Largier, J. L. (1997) Upwelling shadows as nearshore retention sites: The example of northern Monterey Bay. *Cont. Shelf Res.*, **17**, 509–532.

Graham, W. M., Pagès, F. and Hamner, W. M. (2001) A physical context for gelatinous zooplankton aggregations: a review. *Hydrobiologia*, **451**, 199–212.

Greene, C. H., Landry, M. R. and Monger, B. C. (1986) Foraging behavior and prey selection by the ambush entangling predator *Pleurobrachia bachei*. *Ecology*, **67**, 1493–1501.

Greve, W. (1970) Cultivation experiments on North Sea ctenophores. *Helgolander Wiss. Meeresunters.*, **20**, 304–317.

Hays, G. C., Kennedy, H. and Frost, B. W. (2001) Individual variability in diel vertical migration of a marine copepod: why some individuals remain at depth when others migrate. *Limnol. Oceanogr.*, **46**, 2050–2054.

Herman, A. W. (1983) Vertical distribution patterns of copepods, chlorophyll, and production in northeastern Baffin Bay. *Limnol. Oceanogr.*, **28**, 709–719.

Holliday, D. V., Donaghay, P. L., Greenlaw, C. F. *et al.* (2003) Advances in defining fine- and micro-scale pattern in marine plankton. *Aquat. Living Resour.*, **16**, 131–136.

Holliday, D. V., Greenlaw, C. F. and Donaghay, P. L. (2010) Acoustic scattering in the coastal ocean at Monterey Bay, CA, USA: fine-scale vertical structures. *Cont. Shelf Res.*, **30**, 81–103.

Holliday, D. V., Pieper, R. E., Greenlaw, C. F. *et al.* (1998) Acoustical sensing of small scale vertical structure in zooplankton assemblages. *Oceanography*, **11**, 18–23.

Jacobsen, H. P. and Norrbin, M. F. (2009) Fine-scale layer of hydromedusae is revealed by video plankton recorder (VPR) in a semi-enclosed bay in northern norway. *Mar. Ecol. Prog. Ser.*, **380**, 129–135.

Jaffe, J. S., Franks, P. J. S. and Leising, A. W. (1998) Simultaneous imaging zooplankton and of phytoplankton zooplankton distributions. *Oceanography*, **11**, 24–29.

Javidpour, J., Molinero, J. C., Lehmann, A. *et al.* (2009) Annual assessment of the predation of *Mnemiopsis leidyi* in a new invaded environment, the kiel fjord (western Baltic Sea): a matter of concern? *J. Plankton Res.*, **31**, 729–738.

Lincoln, J. A., Turner, J. T., Bates, S. S. *et al.* (2001) Feeding, egg production, and egg hatching success of the copepods acartia tonsa and temora longicornis on diets of the toxic diatom *Pseudo-nitzschia* multiseries and the non-toxic diatom *Pseudo-nitzschia pungens*. *Hydrobiologia*, **453454**, 107–120.

Link, J. S. and Ford, M. D. (2006) Widespread and persistent increase of ctenophora in the continental shelf ecosystem off NE USA. *Mar. Ecol. Prog. Ser.*, **320**, 153–159.

Lloyd, M. (1967) Mean crowding. *J. Anim. Ecol.*, **36**, 1–30.

MacIntyre, S., Alldredge, A. L. and Gotschalk, C. C. (1995) Accumulation of marine snow at density discontinuities in the water column. *Limnol. Oceanogr.*, **40**, 449–468.

McManus, M. A., Alldredge, A. L., Barnard, A. H. *et al.* (2003) Characteristics, distribution and persistence of thin layers over a 48 hour period. *Mar. Ecol. Prog. Ser.*, **261**, 1–19.

McManus, M. A., Cheriton, O. M., Drake, P. J. *et al.* (2005) Effects of physical processes on structure and transport of thin zooplankton layers in the coastal ocean. *Mar. Ecol. Prog. Ser.*, **301**, 199–215.

McManus, M. A., Kudela, R. M., Silver, M. W. *et al.* (2008) Cryptic blooms: are thin layers the missing connection? *Estuar. Coast.*, **31**, 396–401.

Mills, C. E. (1984) Density is altered in hydromedusae and ctenophores in response to changes in salinity. *Biol Bull.*, **166**, 206–215.

Monger, B. C., Chinniah-Chandy, S., Meir, E. *et al.* (1998) Sound scattering by the gelatinous zooplankters aequorea victoria and *Pleurobrachia bachei*. *Deep-Sea Res. Pt II*, **45**, 1255–1271.

Neill, W. E. (1990) Induced vertical migration in copepods as a defence against invertebrate predation. *Nature*, **345**, 524–526.

Nielsen, T. G., Kiorboe, T. and Bjornsen, P. K. (1990) Effects of a *Chrysochromulina polylepis* subsurface bloom on the planktonic community. *Mar. Ecol. Prog. Ser.*, **62**, 21–35.

Oviatt, C. A. and Kremer, P. M. (1977) Predation on the ctenophore, *Mnemiopsis leidyi*, by butterfish, peprilus triacanthus, in Narragansett Bay, Rhode Island. *Chesap. Sci.*, **18**, 236–240.

Pennington, T. J. and Chavez, F. P. (2000) Seasonal fluctuations of temperature, salinity, nitrate, chlorophyll and primary production at station H3/M1 over 1989–1996 in Monterey Bay, California. *Deep-Sea Res. Pt II*, **47**, 947–973.

Purcell, J. E. (1991) A review of cnidarians and ctenophores feeding on competitors in the plankton. *Hydrobiologia*, **216217**, 335–342.

Ramp, S. R., Paduan, J. F., Shulman, I. *et al.* (2005) Observations of upwelling and relaxation events in the northern Monterey Bay during august 2000. J. Geophys. Res. C, **110**, 1–21.

Rasband, W. S. (1997–2012) *ImageJ*. U.S. National Institutions of Health. http://imagej.nih.gov/ij/.

R Core Team (2012) R: A language and environment for statistical computing. http://www.R-project.org.

Raskoff, K. A. (2002) Foraging, prey capture, and gut contents of the mesopelagic narcomedusa *Solmissus* spp. (cnidaria: Hydrozoa). *Mar. Biol.*, **141**, 1099–1107.

Rees, J. T. (1978) Laboratory and field studies on *Eutonina indicans* (coelenterata: Hydrozoa), a common leptomedusa of Bodega Bay, California. *Wasmann J. Biol.*, **36**, 201–209.

Reeve, M. R. (1980) Population dynamics of ctenophores in large scale enclosures over several years. In D.C. Smith, YT (ed.), *Nutrition of the Lower Metazoa*. Pergamon, pp. 73–86.

Reeve, M. R., Walter, M. A. and Ikeda, T. (1978) Laboratory studies of ingestion and food utilization in lobate and tentaculate ctenophores. *Limnol. Oceanogr.*, **23**, 740–751.

Rines, J. E. B., McFarland, M. N., Donaghay, P. L. *et al.* (2010) Thin layers and species-specific characterization of the phytoplankton community in Monterey Bay, California, USA. *Cont. Shelf Res.*, **30**, 66–80.

Rosenfeld, L. K., Schwing, F. B., Garfield, N. *et al.* (1994) Bifurcated flow from an upwelling center: a cold water source for Monterey Bay. *Cont. Shelf Res.*, **14**, 931–964.

Ryan, J. P., Fischer, A. M., Kudela, R. M. *et al.* (2009) Influences of upwelling and downwelling winds on red tide bloom dynamics in Monterey Bay, California. *Cont. Shelf Res.*, **29**, 785–795.

Ryan, J. P., McManus, M. A., Paduan, J. D. *et al.* (2008) Phytoplankton thin layers caused by shear in frontal zones of a coastal upwelling system. *Mar. Ecol. Prog. Ser.*, **354**, 21–34.

Sørnes, T. A. and Aksnes, D. L. (2004) Predation efficiency in visual and tactile zooplanktivores. *Limnol. Oceanogr.*, **49**, 69–75.

Stanlaw, K. A., Reeve, M. R. and Walter, M. A. (1981) Growth, food, and vulnerability to damage of the ctenophore mnemiopsis-mccradyi in its early life-history stages. *Limnol. Oceanogr.*, **26**, 224–234.

Sullivan, J. M., Donaghay, P. L. and Rines, J. E. B. (2010) Coastal thin layer dynamics: consequences to biology and optics. *Cont. Shelf Res.*, **30**, 50–65.

Talapatra, S., Hong, J., McFarland, M. *et al.* (2013) Characterization of biophysical interactions in the water column using in situ digital holography. *Mar. Ecol. Prog. Ser.*, **473**, 29–51.

Timmerman, A. H. V. (2012) Hidden thin layers of toxic diatoms in a coastal bay. M.S. Thesis, University of Hawaii, Honolulu, pp. 49.

Timmerman, A. H. V., McManus, M. A., Cheriton, O. M. *et al.* (2013) Hidden thin layers of toxic diatoms in a coastal bay. In Raine, R., Berdalet, E., McManus, MA and Yamazaki, H. (eds), *Deep Sea Research II. Special Issue: Harmful Alglal Blooms in Stratified Systems*, in press.

Toyokawa, M., Toda, T., Kikuchi, T. *et al.* (2003) Direct observations of a dense occurrence of *Bolinopsis infundibulum* (ctenophora) near the seafloor under the oyashio and notes on their feeding behavior. *Deep-Sea Res.*, **50**, 809–813.

Wickham, H. (2009) *Ggplot2: Elegant Graphics for Data Analysis*. Springer, New York.

Wickham, H. (2011) The split-apply-combine strategy for data analysis. *J. Stat. Softw.*, **40**, 1–29.

Wiebe, P. H., Burt, K. H., Boyd, S. H. *et al.* (1976) A multiple opening/closing net and environmental sensing system for sampling zooplankton. *J. Mar. Res.*, **43**, 313–325.

Williamson, C. E. and Stoeckel, M. E. (1990) Estimating predation risk in zooplankton communities: the importance of vertical overlap. *Hydrobiol.*, **198**, 125–131.

Woodson, C. B., Fong, D. A., Moniz, R. J. *et al.* (in revision) Connecting regional and local scale variability in the Monterey Bay. *J. Phys. Oceanogr.*

Woodson, C. B., Washburn, L., Barth, J. A. *et al.* (2009) Northern Monterey Bay upwelling shadow front: observations of a coastally and surface-trapped buoyant plume. *J. Geophys. Res. C*, **114**, C12013.

Wrobel, D. and Mills, C. E. (1998) *Pacific Coast Pelagic Invertebrates: A Guide to the Common Gelatinous Animals*. Sea Challengers and Monterey Bay Aquarium, Monterey, CA.

Zaret, T. M. and Suffern, J. S. (1976) Vertical migration in zooplankton as a predator avoidance mechanism. *Limnol. Oceanogr.*, **21**, 804–813.

Zuur, A. F., Ieno, E. N., Walker, N. J. *et al.* (2009) *Mixed Effect Models and Extensions in Ecology with R*. Springer, New York.